








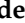


The Retreat of Mountain Glaciers since the Little Ice Age: A Spatially Explicit Database

Silvio Marta ^{1,*}, Roberto Sergio Azzoni ¹, Davide Fugazza ¹, Levan Tielidze ^{2,3}, Pritam Chand ⁴, Katrin Sieron ⁵, Peter Almond ⁶, Roberto Ambrosini ¹, Fabien Anthelme ⁷, Pablo Alviz Gazitúa ⁸, Rakesh Bhambri ⁹, Aurélie Bonin ¹, Marco Caccianiga ¹⁰, Sophie Cauvy-Fraunié ¹¹, Jorge Luis Ceballos Lievano ¹², John Clague ¹³, Justiniano Alejo Cochachín Rapre ¹⁴, Olivier Dangles ¹⁵, Philip Deline ¹⁶, Andre Eger ¹⁷, Rolando Cruz Encarnación ¹⁴, Sergey Erokhin ¹⁸, Andrea Franzetti ¹⁹, Ludovic Gielly ²⁰, Fabrizio Gili ^{1,21}, Mauro Gobbi ²², Alessia Guerrieri ¹, Sigmund Hågvar ²³, Norine Khedim ¹⁶, Rahab Kinyanjui ²⁴, Erwan Messenger ¹⁶, Marco Aurelio Morales-Martínez ⁵, Gwendolyn Peyre ²⁵, Francesca Pittino ¹⁹, Jerome Poulencard ¹⁶, Roberto Seppi ²⁶, Milap Chand Sharma ²⁷, Nurai Urseitova ¹⁸, Blake Weissling ²⁸, Yan Yang ²⁹, Vitalii Zaginaev ¹⁸, Anaïs Zimmer ³⁰, Guglielmina Adele Diolaiuti ¹, Antoine Rabatel ³¹, and Gentile Francesco Ficetola ^{1,20}



Citation: Marta, S.; Azzoni, R.S.; Fugazza, D.; Tielidze, L.; Chand, P.; Sieron, K.; Almond, P.; Ambrosini, R.; Anthelme, F.; Alviz Gazitúa, P.; et al. The Retreat of Mountain Glaciers since the Little Ice Age: A Spatially Explicit Database. *Data* **2021**, *6*, 107. <https://doi.org/10.3390/data6100107>

Academic Editor: Richard Ross Shaker

Received: 31 August 2021
Accepted: 3 October 2021
Published: 9 October 2021

Publisher's Note: MDPI stays neutral with regard to jurisdictional claims in published maps and institutional affiliations.



Copyright: © 2021 by the authors. Licensee MDPI, Basel, Switzerland. This article is an open access article distributed under the terms and conditions of the Creative Commons Attribution (CC BY) license (<https://creativecommons.org/licenses/by/4.0/>).

- ¹ Dipartimento di Scienze e Politiche Ambientali, Università degli Studi di Milano, Via Celoria 10, 20133 Milano, Italy; robertosergio.azzoni@unimi.it (R.S.A.); davide.fugazza@unimi.it (D.F.); roberto.ambrosini@unimib.it (R.A.); bonin.aurelie@gmail.com (A.B.); fabriziogili7@gmail.com (F.G.); alessia.guerrieri@unimi.it (A.G.); guglielmina.diolaiuti@unimi.it (G.A.D.); francesco.ficetola@unimi.it (G.F.F.)
- ² Antarctic Research Centre, Victoria University of Wellington, P.O. Box 600, Wellington 6140, New Zealand; tielidzelevan@gmail.com
- ³ School of Geography, Environment and Earth Sciences, Victoria University of Wellington, P.O. Box 600, Wellington 6140, New Zealand
- ⁴ Department of Geography, School of Environment and Earth Sciences, Central University of Punjab, VPO-Ghudda, Bathinda 151401, Punjab, India; pritamiirs@gmail.com
- ⁵ Centro de Ciencias de la Tierra, Universidad Veracruzana, Xalapa, Veracruz C.P. 91090, Mexico; ksieron@gmail.com (K.S.); marcmorales@uv.mx (M.A.M.-M.)
- ⁶ Department of Soil and Physical Sciences, Lincoln University, Lincoln 7647, New Zealand; peter.almond@lincoln.ac.nz
- ⁷ AMAP, University of Montpellier, IRD, CIRAD, CNRS, INRA, 34090 Montpellier, France; fabien.anthelme@ird.fr
- ⁸ Departamento de Ciencias Biológicas y Biodiversidad, Universidad de Los Lagos, Osorno 5290000, Chile; pablo.alviz@ulagos.cl
- ⁹ Department of Geography, South Asia Institute, Heidelberg University, Voßstraße 2/4130, D-69115 Heidelberg, Germany; rakeshbhambri@gmail.com
- ¹⁰ Dipartimento di Bioscienze, Università degli Studi di Milano, Via Celoria 10, 20133 Milano, Italy; marco.caccianiga@unimi.it
- ¹¹ Centre de Lyon-Villeurbanne, UR RIVERLY, INRAE, 69625 Villeurbanne, France; sophie.cauvy-fraunie@irstea.fr
- ¹² Instituto de Hidrología, Meteorología y Estudios Ambientales IDEAM, Bogotá CP 110911, Colombia; jceballos@ideam.gov.co
- ¹³ Department of Earth Sciences, Simon Fraser University, 8888 University Drive, Burnaby, BC V5A 1S6, Canada; john_clague@sfu.ca
- ¹⁴ Área de Evaluación de Glaciares y Lagunas, Autoridad Nacional del Agua, Huaraz 02002, Peru; jcochachin@ana.gob.pe (J.A.C.R.); rcruz@ana.gob.pe (R.C.E.)
- ¹⁵ CEFÉ, University Montpellier, CNRS, EPHE, IRD, University Paul Valéry Montpellier 3, 34199 Montpellier, France; olivier.dangles@ird.fr
- ¹⁶ Université Savoie Mont Blanc, Université Grenoble Alpes, EDYTEM, 73000 Chambéry, France; philip.deline@univ-smb.fr (P.D.); norine.khedim@univ-smb.fr (N.K.); erwan.messenger@univ-smb.fr (E.M.); jerome.poulencard@univ-smb.fr (J.P.)
- ¹⁷ Mannaki Whenua—Landcare Research, Soils and Landscapes, 54 Gerald St, Lincoln 7608, New Zealand; egera@landcareresearch.co.nz
- ¹⁸ Institute of Water Problems and Hydro-Energy, Kyrgyz National Academy of Sciences, Frunze 533, Bishkek 720033, Kyrgyzstan; erochin@list.ru (S.E.); nurai.urseitova@gmail.com (N.U.); zagivijob@gmail.com (V.Z.)
- ¹⁹ Department of Earth and Environmental Sciences (DISAT), University of Milano-Bicocca, 20126 Milano, Italy; andrea.franzetti@unimib.it (A.F.); francesca.pittino@unimib.it (F.P.)

- ²⁰ Laboratoire d'Écologie Alpine, University Grenoble Alpes, University Savoie Mont Blanc, CNRS, LECA, 38610 Grenoble, France; ludovic.gielly@univ-grenoble-alpes.fr
- ²¹ Department of Life Sciences and Systems Biology, University of Turin, Via Accademia Albertina 13, 10123 Turin, Italy
- ²² Section of Invertebrate Zoology and Hydrobiology, MUSE-Science Museum, Corso del Lavoro e della Scienza, 3, 38122 Trento, Italy; mauro.gobbi@muse.it
- ²³ Department of Ecology and Natural Resource Management (INA), Norwegian University of Life Sciences, Universitetstunet 3, 1433 Ås, Norway; sigmund.hagvar@nmbu.no
- ²⁴ Palynology and Paleobotany Section, Earth Sciences Department, National Museums of Kenya, P.O. Box 40568, Nairobi 00100, Kenya; rkinyanjui@museums.or.ke
- ²⁵ Department of Civil and Environmental Engineering, University of the Andes, Bogotá 111711, Colombia; gf.peyre@uniandes.edu.co
- ²⁶ Department of Earth and Environmental Sciences, University of Pavia, Via Ferrata 1, 27100 Pavia, Italy; roberto.seppi@unipv.it
- ²⁷ Centre for the Study of Regional Development, School of Social Sciences, Jawaharlal Nehru University, New Mehrauli Road, New Delhi 110067, India; milap@mail.jnu.ac.in
- ²⁸ Department of Geological Sciences, University of Texas-San Antonio, Flawn Science Building (FLN), San Antonio, TX 78249, USA; Blake.Weissling@utsa.edu
- ²⁹ Institute of Mountain Hazards and Environment, Chinese Academy of Sciences, Chengdu 610041, China; yyang@imde.ac.cn
- ³⁰ Department of Geography and the Environment, University of Texas at Austin, Austin, TX 78712, USA; anais.zimmer@utexas.edu
- ³¹ University Grenoble Alpes, CNRS, IRD, Grenoble-INP, Institut des Géosciences de l'Environnement (IGE, UMR 5001), 38000 Grenoble, France; antoine.rabatel@univ-grenoble-alpes.fr
- * Correspondence: silvio.marta@hotmail.it

Abstract: Most of the world's mountain glaciers have been retreating for more than a century in response to climate change. Glacier retreat is evident on all continents, and the rate of retreat has accelerated during recent decades. Accurate, spatially explicit information on the position of glacier margins over time is useful for analyzing patterns of glacier retreat and measuring reductions in glacier surface area. This information is also essential for evaluating how mountain ecosystems are evolving due to climate warming and the attendant glacier retreat. Here, we present a non-comprehensive spatially explicit dataset showing multiple positions of glacier fronts since the Little Ice Age (LIA) maxima, including many data from the pre-satellite era. The dataset is based on multiple historical archival records including topographical maps; repeated photographs, paintings, and aerial or satellite images with a supplement of geochronology; and own field data. We provide ESRI shapefiles showing 728 past positions of 94 glacier fronts from all continents, except Antarctica, covering the period between the Little Ice Age maxima and the present. On average, the time series span the past 190 years. From 2 to 46 past positions per glacier are depicted (on average: 7.8).

Dataset: 10.6084/m9.figshare.13700215

Dataset License: CC-BY-4.0

Keywords: glacier retreat; climate change; little ice age; pre-satellite era; global scale

1. Summary

Most of the world's mountain glaciers have been losing mass since the second half of 19th century due to the rise of global temperature [1]. Glacier retreat is evident on all continents, and the rate of retreat has accelerated during recent decades [2–4]. In the European Alps, for example, glaciers have lost 25–30% of their surface area over the past 60 years, and the rate of ice loss is accelerating rapidly—it has been 200–300% faster in the past two decades than 40 years ago [5–7], and similar rates of retreat have been measured in other areas of the world [8]. The biotic and abiotic consequences of glacier retreat have received increasing attention in recent years, with research focusing on the

biotic colonization, the formation and evolution of soils along glacier forelands, and the geomorphological hazards related to deglaciation [9–14], as well as on the impacts of glacier retreat on meltwater availability and human wellbeing [15,16]. In this context, broad-scale, spatially explicit information on the dynamics of glacier retreat is essential to assess the ecological dynamics of biotic colonization across multiple regions and to develop adequate adaptation and mitigation strategies to reduce geomorphological risks and cope with meltwater scarcity in arid regions.

Several databases summarizing information on glacier retreat are currently available (e.g., World Glacier Monitoring Service [17] and Global Land Ice Measurements from Space [18,19]). In most cases, they provide recent outlines obtained through remote sensing. For some glaciers, the GLIMS initiative also provides past outlines, such as glacier extent at the end of the Little Ice Age (LIA). However, these databases generally do not provide information on glacier extent at multiple time points, covering the retreat occurring during the last century. For many glaciers, high-quality data on margins are available since the end of the LIA (from the late 19th century in part of Northern Europe, to as early as the 17th–18th century in other mountain ranges such as the tropical Andes; see e.g., [20]). These data have been obtained through geomorphologic analyses mainly based on morpho-stratigraphic positions, morphology, and relationships of moraines which is further dated by in situ relative and absolute dating methods (e.g., radiocarbon, lichenometry, dendrochronology, optically stimulated luminescence, and terrestrial cosmogenic nuclide dating), analysis of old/repeated photographs and paintings, historical archives and maps including topographical maps, and remotely sensed data [21–24]. The data are typically analyzed using multi-data integrative methods and summarized in long multi-temporal retreat maps. However, because they are derived from disparate sources, the data require manual processing for analysis and presentation. As a consequence, such datasets are mainly available fragmentally for some specific glaciers and for some restricted areas. Thus, there is a need to synthesize such long multi-temporal glacier fluctuation datasets from all over the world to develop spatially explicit datasets showing positions of glacier fronts since the Little Ice Age (LIA) maxima at one place.

We focused on time-series of glacier margins from the LIA maximum extent to the present, with representative examples from the major mountain ranges of the world, except Antarctica. We performed a literature search of glaciers with well-documented retreat series worldwide (i.e., long and spatially explicit time series of glacier margins); the dataset was further complemented with data from several alternative sources (i.e., topographic maps, historical images, and drawings), field work, and remotely sensed data. We focused on mountain glaciers (see [25] for definitions), even though our dataset also included a few glaciers that are linked to icecaps in Iceland and Greenland (Figure 1).

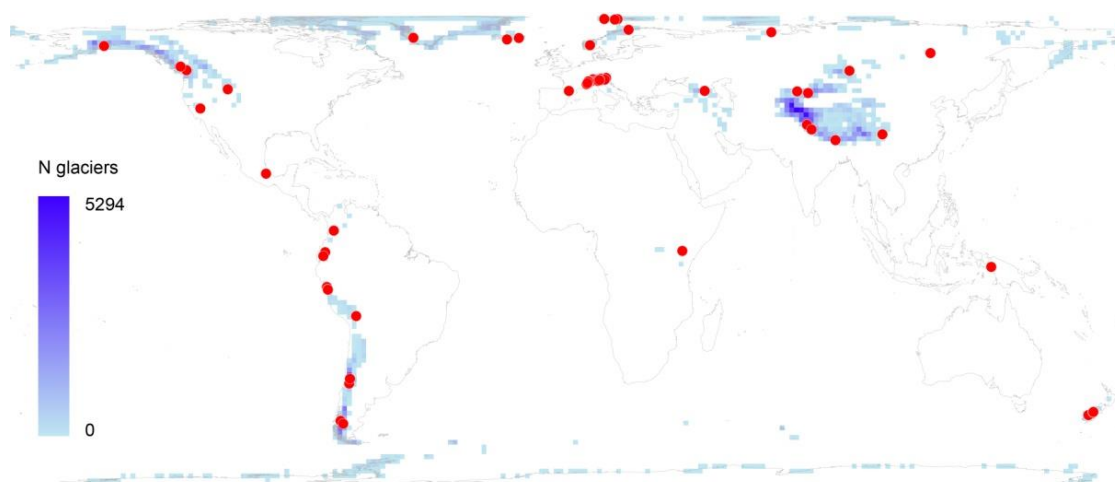


Figure 1. Distribution of glaciers included in the dataset (red dots). Due to proximity, some dots are superimposed. The blue shaded areas show the number of extant glaciers for $1.5^\circ \times 1.5^\circ$ cells (source: [18,19]).

The dataset includes dated margins for 94 glaciers from all the continents except Antarctica (Figure 1). From 2 to 46 past positions are included (average: 7.8 lines per glacier); at least four past positions are shown for 97% of the glaciers. In total, we provide 728 glacier outlines and/or frontal positions for the period from the 16th century to the present. The average length of the time series is 188 years; the length is ≥ 85 years for 94% of the glaciers. About 97% of the glacier margins date to the period from the 19th century to today, with a marked increase of data over the second half of the 20th century (Figure 2). The oldest outlines are largely restricted to areas where researchers have dated the LIA maximum back to the 16th–18th centuries (e.g., South America [26,27]).

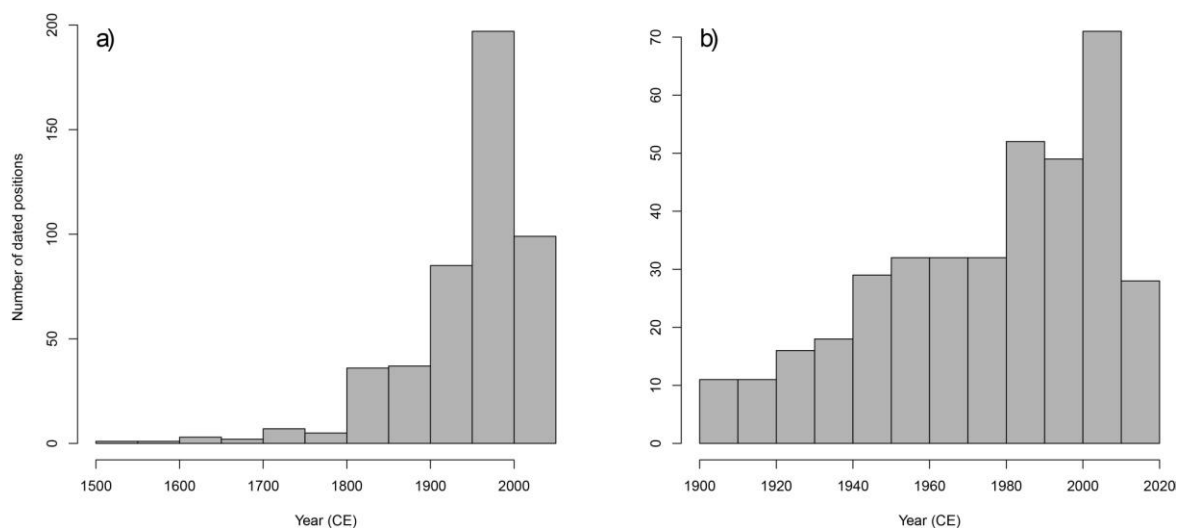


Figure 2. Temporal distribution of glacier margins in the dataset. (a) All margins and (b) 20th and 21st century margins. CE: Common Era.

Although the dataset includes glaciers from all continents (Figure 1), there are differences in coverage among areas, as observed for other environmental datasets [28,29]. Specifically, 35% of the data are from Europe (including Svalbard); 29% are from Asia (including Papua New Guinea); 15% from South America; 11% from Northern and Central America, 8% from Oceania (New Zealand); and 2% are from Africa. Our primary objective was not to obtain a complete, global scale dataset with equal coverage from all the continents, but instead to collate high-quality data with multiple positions from several glaciers around the world. We encourage users to add to our dataset information from additional glaciers.

The present work is part of the European Community's Horizon 2020 project IceCommunities (Grant Agreement no. 772284). IceCommunities combines innovative methods and a global approach to boosting our understanding of the evolution of ecosystems in recently deglaciated areas. IceCommunities investigates chronosequences ranging from recently deglaciated terrains to late successional stages of soil pedogenesis. Through environmental DNA metabarcoding IceCommunities identifies taxa from multiple taxonomic groups (bacteria, fungi, protists, soil invertebrates, and plants), to obtain a complete reconstruction of biotic communities along glacier forelands over multiple mountain areas across the globe and to measure the rate of colonization at an unprecedented level of detail. Information on assemblages is then combined with analyses of soil, landscape, and climate to identify the drivers of community change. IceCommunities also assesses the impact of ecogeographical factors (climate and the regional pool of potential colonizers) on colonization. Analyses of functional traits are also used to reconstruct how functional diversity emerges during community formation, and how it scales to the functioning of food webs. IceCommunities will help to predict the future development of these increasingly

important ecosystems, providing a supported rationale for the appropriate management of these areas.

2. Data Description

The dataset is downloadable from <https://doi.org/10.6084/m9.figshare.13700215> (accessed on 4 October 2021). It contains the following data files (Tables 1–4):

Table 1. Description of the datasets.

Filename	Description
IC_glac_lines (* .shp, * .shx, * .prj, * .dbf)	ESRI shapefile (EPSG:4326) containing the 728 reconstructed positions of glacier margins for the 94 glacier analyzed. For each line, glacier name, dating, source, GLIMS id, and maximum extent are reported in the associated table.
IC_glac_sites (* .csv)	Table reporting the description of the study sites (glacier name, GLIMS id, country, coordinates of the centroid, mean elevation, mean annual temperature, annual precipitation, lithology, area, and number of reconstructed lines)
IC_glac_references (* .csv)	Table reporting the references cited in IC_glac_lines

IC_glac_lines

Table 2. Variable identities, definitions, and attributes for the dataset IC_glac_lines.

Identity	Definition	Unit	Storage	Range
glacier	Glacier name	-	Character	-
dating	Dating	year CE	Integer/character	1500 to 2019
source	Reference	-	Character	-
GLIMS_id	Id	-	Character	-
max_extent	Maximum glacier extent ¹	-	Character (y/n)	-

¹ For each glacier, “y” identifies the margin(s) at LIA maximum. The information is missing (i.e., all “n”) when the reconstructed series is incomplete (e.g., Brewster glacier: 1986–2011).

IC_glac_sites

Table 3. Variable identity, definition, and attributes for the dataset IC_glac_sites.

Identity	Definition	Unit	Storage	Range
glacier	Glacier name	-	Character	-
country	Country name	-	Character	-
GLIMS_id	Id	-	Character	-
lon_wgs84	Longitude (centroid)	DD	Numeric	−149.631 to 170.173
lat_wgs84	Latitude (centroid)	DD	Numeric	−47.530 to 78.899
elev_m	Mean elevation	m a.s.l.	Integer	51 to 5120
mat_°C	Mean annual temperature ¹	°C	Numeric	−13.28 to 9.49
pcp_mm	Annual precipitation ¹	mm	Integer	181 to 4515
litho	Lithology ²	-	Character	-
area_km2	Glacier area ³	km ²	Numeric	0.014 to 8091.670
N_positions	Number of reconstructed lines	-	Numeric	1 to 27

¹ Retrieved from CHELSA [30]. ² Codes identifying lithology refer to the lithological classes used in Hartmann and Moosdorf [31]. Specifically: mt, metamorphics; ss, siliciclastic sedimentary rocks; pa, acid plutonic rocks; su, unconsolidated sediments; pb, basic plutonic rocks; va, acid volcanic rocks; sc, carbonate sedimentary rocks; vb, basic volcanic rocks; sm, mixed sedimentary rocks; and vi, intermediate volcanic rocks. ³ Most-recent available estimate; retrieved from GLIMS database v20200630 [18,19].

IC_glac_references

Table 4. Variable identity, definition, and attributes for the dataset IC_glac_references.

Identity	Definition	Unit	Storage	Range
References	Sources used to reconstruct or date glacier margins	-	Character	-

3. Methods

We focused on time-series of glacier margins from the LIA maximum extent to the present, with representative examples from the major mountain ranges of the world, except Antarctica. We first performed a literature search of glaciers for which there are long and spatially explicit time series of glacier margins. Data from the literature were complemented with new data, obtained mostly from topographic maps; historical, aerial, and satellite images; and field surveys. Some of the glacier margins and dates are based on our measurements made in the field. Older positions are based mainly on moraines that are clearly visible on images and in the field, and have been dated using lichenometry, dendrochronology, radiocarbon, and cosmogenic nuclides. The reconstruction of LIA maxima and subsequent glacier extent have been carried out differently by different studies, in most of cases using a multi-data layer integration approach (MDIA, [32]). This approach incorporates individual layers of information extracted from geomorphological mapping, analysis of photo sequences, historical archives, maps inferences, and hillshade DEM analysis into a GIS environment. For many glaciers, glacial geomorphological evidence and landforms (e.g., lateral, recessional, and hummocky moraines, supraglacial morainic ridges, trim lines, and palaeo-channels) resultant due to LIA glaciation and latterly molded by deglaciation are initially mapped using high-resolution remote sensing images and DEMs and further validated in the field. These data are integrated with sequences of pictures taken in the field in different times, or obtained from satellite/aerial images. Moreover, additional information on the historical terminus, surface characteristics, and the extents of individual glaciers was extracted from historical descriptions, documents, and maps preserved since LIA maxima, and existing marks in the field. All the spatial data were integrated into a spatial database, and the output was further validated against known LIA positions from available regional chronologies (e.g., [26]).

We used four approaches to validate the dated margins for each glacier: (i) we performed a double-check against the original publication; (ii) each shapefile was checked by more than two co-authors, to confirm the consistence across areas of the world; (iii) the database was reviewed by regional experts, i.e., by researchers experienced in the geomorphology and mapping of glaciated areas of a study region; and (iv) we then performed a final check based on available high resolution satellite images in Google Earth.

Images were georeferenced and lines were digitized using QGIS 3.4.12; additional analyses were performed using R 4.0.5.

4. User Notes

The final dataset is provided in ESRI shapefile format (WGS 84, decimal degrees—EPSG:4326). Missing/anomalous data are present in both IC_glac_lines and IC_glac_sites. They refer to some GLIMS IDs lacking (glacier not in the references database or extinct). Additionally, it was not always possible to obtain precise datings for the glacier margins, particularly those older than the first half of the 20th century (marked as “NA”, “LIA”, “M2”, or “M3” and “(estimated- . . .)”). Sources of uncertainty included the following:

(1) For a number of glaciers, dating of old margins were based on published geomorphological chronologies of the region, rather than on the glacier itself. For example, LIA moraines in the Peruvian Andes, although clearly visible in the field, have not been directly dated for all the glaciers, therefore we assume ages similar to those of nearby glaciers [25]. Similarly, in the absence of direct dating, we assume that LIA moraines of glacier margins

in the European Alps date to the last half of the 19th century, even though some variation might exist among glaciers due to their different response time [33]. Cases with large age uncertainties are explicitly acknowledged in the dataset.

(2) Even if a moraine has been directly dated (e.g., using lichenometry or radiocarbon dating), the user must be aware that every technique has inherent uncertainties. The user should refer to the reference(s) cited in the dataset for further information on this uncertainty.

(3) Finally, some level of spatial uncertainty exists, for instance when data are based on old maps or images, mostly because of their limited quality and/or spatial resolution.

Author Contributions: Conceptualization, G.F.F., A.R., G.A.D. and S.M.; methodology, S.M., R.S.A., D.F., L.T., P.C. and K.S.; software, S.M.; validation, all the authors; formal analysis, S.M., R.S.A., D.F., L.T., P.C. and K.S.; investigation, S.M., R.S.A., D.F., L.T., P.C. and K.S.; resources, all the authors; data curation, S.M. and D.F.; writing—original draft preparation, G.F.F. and S.M.; writing—review and editing, all the authors; visualization, S.M.; supervision, G.F.F., A.R. and G.A.D.; project administration, G.F.F.; funding acquisition, G.F.F., A.R. and J.P. All authors have read and agreed to the published version of the manuscript.

Funding: This study was supported by the European Research Council under the European Community's Horizon 2020 Programme, Grant Agreement no. 772284 (IceCommunities) and supported by the National Natural Science Foundation of China (Grant No.41861134039, No.41941015). A. Rabatel, G.F. Fictola, J. Poulencard, and L. Gielly acknowledge the support of Labex OSUG@2020 (*Investissements d'avenir*, ANR10 LABX56) and the French *Service National d'Observation* GLACIOCLIM (UGA, CNRS INSU, IRD, IPEV, and INRAE). P. Chand acknowledges the financial support of the Science and Engineering Research Board (SERB), New Delhi (India) vide SERB Project No. PDF/2017/002717 (NPDF Scheme).

Institutional Review Board Statement: Not applicable.

Informed Consent Statement: Not applicable.

Data Availability Statement: The data presented in this study are openly available in FigShare doi:10.6084/m9.figshare.13700215.

Conflicts of Interest: The authors declare no conflict of interest.

References

1. Marzeion, B.; Cogley, J.G.; Richter, K.; Parkes, D. Attribution of global glacier mass loss to anthropogenic and natural causes. *Science* **2014**, *345*, 919–921. [[CrossRef](#)] [[PubMed](#)]
2. Zemp, M.; Huss, M.; Thibert, E.; Eckert, N.; McNabb, R.; Huber, J.; Barandun, M.; Machguth, H.; Nussbaumer, S.U.; Gärtner-Roer, I.; et al. Global glacier mass changes and their contributions to sea-level rise from 1961 to 2016. *Nature* **2019**, *568*, 382–386. [[CrossRef](#)] [[PubMed](#)]
3. Leclercq, P.W.; Oerlemans, J.; Cogley, J.G. Estimating the Glacier Contribution to Sea-Level Rise for the Period 1800–2005. *Surv. Geophys.* **2011**, *32*, 519–535. [[CrossRef](#)]
4. Hock, R.; Rasul, G.; Adler, C.; Cáceres, B.; Gruber, S.; Hirabayashi, Y.; Jackson, M.; Käab, A.; Kang, S.; Kutuzov, S.; et al. High Mountain Areas. In *IPCC Special Report on the Ocean and Cryosphere in a Changing Climate*; Pörtner, H.-O., Roberts, D.C., Masson-Delmotte, V., Zhai, P., Tignor, M., Poloczanska, E., Mintenbeck, K., Alegria, A., Nicolai, M., Okem, A., et al., Eds.; IPCC Intergovernmental Panel on Climate Change: Geneva, Switzerland. Available online: www.ipcc.ch/2019 (accessed on 2 August 2021).
5. Gardent, M.; Rabatel, A.; Dedieu, J.-P.; Deline, P. Multitemporal glacier inventory of the French Alps from the late 1960s to the late 2000s. *Glob. Planet. Chang.* **2014**, *120*, 24–37. [[CrossRef](#)]
6. Smiraglia, C.; Diolaiuti, G.A. *The New Italian Glacier Inventory*; Ev-K2-CNR: Bergamo, Italy, 2015.
7. Paul, F.; Rastner, P.; Azzoni, R.S.; Diolaiuti, G.; Fugazza, D.; Le Bris, R.; Nemec, J.; Rabatel, A.; Ramusovic, M.; Schwaizer, G.; et al. Glacier shrinkage in the Alps continues unabated as revealed by a new glacier inventory from Sentinel-2. *Earth Syst. Sci. Data* **2020**, *12*, 1805–1821. [[CrossRef](#)]
8. Tielidze, L.G.; Wheate, R.D. The Greater Caucasus Glacier Inventory (Russia, Georgia and Azerbaijan). *Cryosphere* **2018**, *12*, 81–94. [[CrossRef](#)]
9. Khedim, N.; Cecillon, L.; Poulencard, J.; Barré, P.; Baudin, F.; Marta, S.; Rabatel, A.; Dentant, C.; Cauvy-Fraunié, S.; Anthelme, F.; et al. Topsoil organic matter build-up in glacier forelands around the world. *Glob. Chang. Biol.* **2021**, *27*, 1662–1677. [[CrossRef](#)]
10. Cauvy-Fraunié, S.; Dangles, O. A global synthesis of biodiversity responses to glacier retreat. *Nat. Ecol. Evol.* **2019**, *3*, 1675–1685. [[CrossRef](#)]

11. Erschbamer, B.; Caccianiga, M. Glacier Forelands: Lessons of Plant Population and Community Development. *Prog. Bot.* **2016**, *78*, 259–284. [[CrossRef](#)]
12. Ficetola, G.F.; Marta, S.; Guerrieri, A.; Gobbi, M.; Ambrosini, R.; Fontaneto, D.; Zerboni, A.; Poulenard, J.; Caccianiga, M.; Thuiller, W. Dynamics of ecological communities following current retreat of glaciers. *Annu. Rev. Ecol. Evol. Syst.* **2021**, *52*. [[CrossRef](#)]
13. Rosero, P.; Crespo-Pérez, V.; Espinosa, R.; Andino, P.; Barragán, Á.; Moret, P.; Gobbi, M.; Ficetola, G.F.; Jaramillo, R.; Muriel, P.; et al. Multi-taxa colonisation along the foreland of a vanishing equatorial glacier. *Ecography* **2021**, *44*, 1010–1021. [[CrossRef](#)]
14. Carey, M. Living and dying with glaciers: People's historical vulnerability to avalanches and outburst floods in Peru. *Glob. Planet. Chang.* **2005**, *47*, 122–134. [[CrossRef](#)]
15. Carey, M. The history of ice: How glaciers became an endangered species. *Environ. Hist.* **2007**, *12*, 497–527. [[CrossRef](#)]
16. Nüsser, M.; Schmidt, S. Nanga Parbat revisited: Evolution and dynamics of sociohydrological interactions in the Northwestern Himalaya. *Ann. Am. Assoc. Geogr.* **2017**, *107*, 403–415. [[CrossRef](#)]
17. WGMS. *Fluctuations of Glaciers Database*; World Glacier Monitoring Service: Zurich, Switzerland. [[CrossRef](#)]
18. GLIMS; NSIDC. *Global Land Ice Measurements from Space Glacier Database*; International GLIMS Community and the National Snow and Ice Data Center: Boulder, CO, USA, 2005. Available online: www.glims.org (accessed on 3 February 2021).
19. Raup, B.H.; Racoviteanu, A.; Khalsa, S.J.S.; Helm, C.; Armstrong, R.; Arnaud, Y. The GLIMS Geospatial Glacier Database: A New Tool for Studying Glacier Change. *Glob. Planet. Chang.* **2007**, *56*, 101–110. [[CrossRef](#)]
20. Rabatel, A.; Francou, B.; Soruco, A.; Gomez, J.; Cáceres, B.; Ceballos, J.L.; Basantes, R.; Vuille, M.; Sicart, J.E.; Huggel, C.; et al. Current state of glaciers in the tropical Andes: A multi-century perspective on glacier evolution and climate change. *Cryosphere* **2013**, *7*, 81–102. [[CrossRef](#)]
21. Nussbaumer, S.U.; Zumbühl, H.J. The Little Ice Age history of the Glacier des Bossons (Mont Blanc massif, France): A new high-resolution glacier length curve based on historical documents. *Clim. Chang.* **2012**, *111*, 301–334. [[CrossRef](#)]
22. Zumbühl, H.J.; Nussbaumer, S.U. Little Ice Age glacier history of the Central and Western Alps from pictorial documents. *Cuad. Investig. Geogr.* **2018**, *44*, 115–136. [[CrossRef](#)]
23. Nüsser, M.; Schmidt, S. Glacier changes on the Nanga Parbat 1856–2020: A multi-source retrospective analysis. *Sci. Total Environ.* **2021**, *785*, 147321. [[CrossRef](#)]
24. Nüsser, M.; Schmidt, S. Assessing glacier changes in the Nanga Parbat region using a multitemporal photographic dataset. *Data Brief* **2021**, *37*, 107178. [[CrossRef](#)] [[PubMed](#)]
25. Cogley, J.G.; Arendt, A.A.; Bauder, A.; Braithwaite, R.J.; Hock, R.; Jansson, P.; Kaser, G.; Moller, M.; Nicholson, L.; Rasmussen, L.A.; et al. *Glossary of Glacier Mass Balance and Related Terms*; IHP-VII Technical Documents in Hydrology No. 86; IACS Contribution No. 2; UNESCO-IHP: Paris, France, 2011.
26. Jomelli, V.; Favier, V.; Rabatel, A.; Brunstein, D.; Hoffmann, G.; Francou, B. Fluctuations of glaciers in the tropical Andes over the last millennium and palaeoclimatic implications: A review. *Paleogeogr. Paleoclimatol. Paleoecol.* **2009**, *281*, 269–282. [[CrossRef](#)]
27. Morano-Buchner, C.; Aravena, J.C. Lichenometric analysis using genus *Rhizocarpon*, section *Rhizocarpon* (Lecanorales: Rhizocarpaceae) at Mount San Lorenzo, southern Chile. *Rev. Chil. Hist. Nat.* **2013**, *86*, 465–473. [[CrossRef](#)]
28. Martin, L.J.; Blossey, B.; Ellis, E. Mapping where ecologists work: Biases in the global distribution of terrestrial ecological observations. *Front. Ecol. Environ.* **2012**, *10*, 195–201. [[CrossRef](#)]
29. Ficetola, G.F.; Rondinini, C.; Bonardi, A.; Katariya, V.; Padoa-Schioppa, E.; Angulo, A. An evaluation of the robustness of global amphibian range maps. *J. Biogeogr.* **2014**, *41*, 211–221. [[CrossRef](#)]
30. Karger, D.N.; Conrad, O.; Böhrer, J.; Kawohl, T.; Kreft, H.; Soria-Auza, R.W.; Zimmermann, N.E.; Linder, H.P.; Kessler, M. Climatologies at high resolution for the earth's land surface areas. *Sci. Data* **2017**, *4*, 170122. [[CrossRef](#)] [[PubMed](#)]
31. Hartmann, J.; Moosdorf, N. The new global lithological map database GLiM: A representation of rock properties at the Earth surface. *Geochem. Geophys. Geosyst.* **2012**, *13*, Q12004. [[CrossRef](#)]
32. Chand, P.; Sharma, M.C.; Bhambri, R.; Sangewar, C.V.; Juyal, N. Reconstructing the pattern of the Bara Shigri Glacier fluctuation since the end of the Little Ice Age, Chandra valley, north-western Himalaya. *Prog. Phys. Geogr.* **2017**, *41*, 643–675. [[CrossRef](#)]
33. Zekollari, H.; Huss, M.; Farinotti, D. On the Imbalance and Response Time of Glaciers in the European Alps. *Geophys. Res. Lett.* **2020**, *47*, e2019GL085578. [[CrossRef](#)]